DSN Station Locations and Uncertainties

W. M. Folkner
Tracking Systems and Applications Section

Accurate spacecraft navigation using radio metric data requires knowledge of the locations of the tracking stations. Through analysis of a variety of space–geodetic data, the locations of many DSN antennas are known with centimeter-level accuracy. Newer DSN antennas have had their positions determined by a combination of Global Positioning System measurements and conventional survey, with decimeter-level accuracy. The locations of the DSN antennas are given, in a reference frame consistent with the Earth orientation calibrations routinely delivered to navigation teams. The uncertainties in the antenna locations are also described.

I. Introduction

Radio metric data, particularly two-way coherent Doppler and range, have been used to navigate robotic spacecraft since the inception of planetary exploration. For a spacecraft in interplanetary cruise or transit, much of the information content inherent in the data for position determination comes from the signature in the spacecraft radio signal frequency, as received by an Earth tracking station, imposed by the Earth's rotation [1–3]. The diurnal signature in the radio metric data yields information about the right ascension and declination of the spacecraft with respect to the direction of the Earth's spin axis at the time of observation. The locations of the tracking antennas, as well as the orientation of the Earth as a function of time, must be known in order to effectively utilize the radio metric data to deduce the spacecraft position with respect to a target body.

The relative locations of many antennas have been determined by very long baseline interferometry (VLBI), a technique also used to monitor the orientation of the Earth [e.g., 4,5]. The VLBI data measure the difference in time of arrival of signals from extragalactic radio sources. The difference in arrival time can be used to solve for the difference in antenna locations as well as Earth orientation and the positions of the radio sources. The VLBI measurements are not sensitive to a translation common to all antenna positions, so other information is needed to determine the locations with respect to the Earth's center of mass.

Satellite laser ranging (SLR) and Global Positioning System (GPS) measurements determine the range between tracking stations and Earth-orbiting satellites. These measurements are sensitive to both the locations of the tracking stations and, through the satellite orbit, the Earth's center of mass. Careful surveys between nearby SLR, GPS, and/or VLBI tracking stations allow comparison between the techniques. Comparisons of station locations determined by different geodetic techniques show consistency at the few-mm level, after overall translations and rotations are removed [6]. Comparisons between GPS and SLR station determinations show agreement on the location of the geocenter to about 1 cm. The

comparisons also allow the determination of geocentric station locations for VLBI antennas that are not co-located with GPS or SLR stations.

Some of the DSN antennas have participated in VLBI measurements. The estimated station locations and uncertainties of these antennas, as derived from analysis of these VLBI measurements, are reported to the International Earth Rotation Service (IERS) [7]. The IERS compares the estimated positions with positions estimated using other space–geodetic techniques. The IERS then publishes a set of locations of all contributing stations, including the participating DSN stations [6]. DSN antennas that have not participated in VLBI measurements have had their positions determined by a combination of GPS measurements and conventional survey measurements. If necessary, this combination of measurements can be used to determine locations with cm-level accuracy. However, since 15-cm or better accuracy is sufficient to meet expected mission navigation requirements, the survey measurements of the DSN antennas were made with few-cm accuracy.

The station locations of all current DSN antennas are given below. The 34-m beam-waveguide (BWG) antenna under construction at Madrid is the only antenna whose position has not been established with decimeter accuracy. There are plans to acquire the necessary survey information later in the construction process.

II. The Coordinate System

To use station locations with submeter accuracy, it is necessary to define clearly a coordinate system. In the past, there have been many different local coordinate systems and many different Earth geoids used to express latitudes and longitudes. This has led to much confusion in the transformation of coordinates. The IERS has established a terrestrial reference frame for comparisons of station locations with cm-level accuracy. The IERS also maintains a celestial reference frame and coordinates delivery of Earth orientation measurements that describe the orientation of station locations in inertial space.

The IERS issues a list of station locations each year. The coordinate system has been changing slowly as the data have improved and as ideas about how to best define the coordinate system have developed. The overall changes from year to year have been at the few-cm level. Thus, it is not enough simply to specify consistency with the IERS Terrestrial Reference Frame (ITRF), but a particular version must be specified. This article is based on the 1993 version of the ITRF, namely ITRF93 [8]. Earlier versions of the ITRF were known to be inconsistent (at the 1- to 3-cm level) with the Earth orientation distributions. The 1993 version of the ITRF (ITRF93) was different from earlier versions of the ITRF in that it was defined to be consistent with the distributed Earth orientation determinations. Later realizations of the ITRF also differ from ITRF93 coordinates, since the IERS has chosen to align ITRF94 and ITRF95 with ITRF92. For most DSN users, it will be slightly advantageous to have ITRF93 coordinates that are consistent with the Earth orientation series.[1] Users interested in precise comparisons with other systems should keep in mind the small systematic differences.

The ITRF93 is listed only in Cartesian coordinates (x-, y-, and z-coordinates). This avoids the potential for confusion among the various geoid definitions. Cartesian coordinates are adopted as the fundamental coordinates in this article. Since many users would prefer geodetic coordinates, a list of geodetic coordinates also is given. The geodetic coordinates are derived from the Cartesian coordinates by the method described in IERS Technical Note 13 [9], using an equatorial radius of 6378136.3 m and a flattening factor of $f = 298.257$.

[1] The IERS has announced plans to change Earth orientation deliveries, starting January 1, 1997, to make the Earth orientation series consistent with the current definitions of the terrestrial and celestial reference frames. Since the IERS has not yet made this change, and has not announced specific algorithms for doing so, JPL plans to maintain production of Earth orientation products, for DSN users, consistent with ITRF93 definitions.

III. Station Locations

Table 1 gives the Cartesian coordinates of the current DSN station locations in the ITRF93 reference system. Table 2 gives a list of geodetic coordinates. Because continental drift changes station locations by several cm per year, it is necessary to specify the reference time for the station locations. The locations given in Tables 1 and 2 are for the epoch 1993.0. To transform to any other epoch, the site velocities should be used. Table 3 gives the ITRF93 site velocities for the DSN sites, in both Cartesian and east–north–vertical components.

The reference points for the locations in Tables 1 and 2 are the effective intersection of axes. For antennas whose axes do not intersect, the effective intersection of axes is typically the center of the lower axis. The reference point for each antenna is described in Appendix A. Also given in Appendix A is information about how the position of each antenna was derived. This is included so that with future information the station locations can be improved and possible discrepancies investigated. In particular, six types of antennas have had the positions with respect to a ground-level monument inferred from construction drawings, which are included for reference. The position uncertainties of these antennas can be reduced significantly, if desired, by making measurements of the vertical offsets.

Table 1. Cartesian coordinates of DSN antennas in the ITRF93 reference frame at epoch 1993.0.

Antenna	X-axis, m	Y-axis, m	Z-axis, m
DSS 12	−2350443.812	−4651980.837	3665630.988
DSS 13	−2351112.491	−4655530.714	3660912.787
DSS 14	−2353621.251	−4641341.542	3677052.370
DSS 15	−2353538.790	−4641649.507	3676670.043
DSS 16	−2354763.158	−4646787.462	3669387.069
DSS 17	−2354730.357	−4646751.776	3669440.659
DSS 23	−2354757.567	−4646934.675	3669207.824
DSS 24	−2354906.495	−4646840.128	3669242.317
DSS 25	−2355022.066	−4646953.636	3669040.895
DSS 26	−2354890.967	−4647166.925	3668872.212
DSS 27	−2349915.260	−4656756.484	3660096.529
DSS 28	−2350101.849	−4656673.447	3660103.577
DSS 33	−4461083.514	2682281.745	−3674570.392
DSS 34	−4461146.756	2682439.293	−3674393.542
DSS 42	−4460981.016	2682413.525	−3674582.072
DSS 43	−4460894.585	2682361.554	−3674748.580
DSS 45	−4460935.250	2682765.710	−3674381.402
DSS 46	−4460828.619	2682129.556	−3674975.508
Parkes	−4554231.843	2816758.983	−3454036.065
DSS 53	4849330.129	−0360338.092	4114758.766
DSS 54	4849519.988	−0360641.653	4114504.590
DSS 61	4849245.211	−0360278.166	4114884.445
DSS 63	4849092.647	−0360180.569	4115109.113
DSS 65	4849336.730	−0360488.859	4114748.775
DSS 66	4849148.543	−0360474.842	4114995.021

Table 2. Geodetic coordinates of DSN antennas in the ITRF93 reference frame at epoch 1993.0.[a]

Station	Latitude			Longitude			Height, m
	deg	min	sec	deg	min	sec	
DSS 12	35	17	59.77577	243	11	40.24697	0962.875
DSS 13	35	14	49.79342	243	12	19.95493	1071.178
DSS 14	35	25	33.24518	243	6	37.66967	1002.114
DSS 15	35	25	18.67390	243	6	46.10495	0973.945
DSS 16	35	20	29.54391	243	7	34.86823	0944.711
DSS 17	35	20	31.83778	243	7	35.38803	0937.650
DSS 23	35	20	22.38335	243	7	37.70043	0946.086
DSS 24	35	20	23.61555	243	7	30.74842	0952.156
DSS 25	35	20	15.40450	243	7	28.69836	0960.862
DSS 26	35	20	08.48213	243	7	37.14557	0970.159
DSS 27	35	14	17.78052	243	13	24.06569	1053.203
DSS 28	35	14	17.78136	243	13	15.99911	1065.382
DSS 33	−35	24	01.76138	148	58	59.12204	0684.839
DSS 34	−35	23	54.53995	148	58	55.06320	0692.750
DSS 42	−35	24	02.44494	148	58	52.55396	0675.356
DSS 43	−35	24	8.74388	148	58	52.55394	0689.608
DSS 45	−35	23	54.46400	148	58	39.65992	0675.086
DSS 46	−35	24	18.05462	148	58	59.08571	0677.551
Parkes	−32	59	54.25297	148	15	48.64683	0415.529
DSS 53	40	25	38.48036	355	45	1.24307	0827.501
DSS 54	40	25	27.75526	355	44	48.99940	0823.939
DSS 61	40	25	43.45508	355	45	3.51113	0841.159
DSS 63	40	25	52.34908	355	45	7.16030	0865.544
DSS 65	40	25	37.86055	355	44	54.88622	0834.539
DSS 66	40	25	47.90367	355	44	54.88739	0850.582

[a] The geoid assumed has an equatorial radius of 6378136.3 m and a flattening factor of $f = 298.257$, as described in IERS Technical Note 13 [9].

Table 3. DSN site velocities in the ITRF93 reference frame.

Station	X-axis, m/yr	Y-axis, m/yr	Z-axis, m/yr	East, m/yr	North, m/yr	Vertical, m/yr
Goldstone	−0.0191	0.0061	−0.0047	−0.0198	−0.0057	−0.0001
Canberra	−0.0354	−0.0017	0.0412	0.0197	0.0506	0.0001
Madrid	−0.0141	0.0222	0.0201	0.0211	0.0255	0.0011

The DSN antennas can be used in a mode where the position of the subreflector is changed as a function of the antenna elevation to compensate for the change in the shape of the antenna. This mode, sometimes referred to as "autofocused," commonly is used for spacecraft telemetry and radio metric tracking. JPL navigation and VLBI data reduction software does not specifically model the motion of the subreflectors when the antennas are autofocused. (This is not a problem when the subreflector is fixed, as is usual for VLBI users.) The motion of the subreflector can be conveniently modeled as a change (reduction) in the vertical component of the station location. This effective vertical offset is 7 cm for the 70-m antennas and 1.5 cm for the 34-m high-efficiency (HEF) antennas.[2] DSN users who use the antennas in the autofocused mode and need cm-level accuracy for these stations must account for this effect.

IV. Station Location Uncertainties

A covariance matrix describing the uncertainties in the DSN station locations has been formed. This covariance matrix is intended for use by spacecraft navigation teams and is expressed in a format suitable for use in the Orbit Determination Program (ODP). The full covariance matrix is given in Appendix B. Table 4 gives the square root of the diagonal elements of the station location covariance expressed in cylindrical coordinates. The coordinate uncertainties in distance from the Earth's spin axis, distance from the equatorial plane (z-height), and longitude are given. The uncertainties in longitude have been converted to meters by multiplying the uncertainties in radians by the distance from the spin axis. Coordinate uncertainties are 3 to 4 cm for stations with positions determined by VLBI measurements. Uncertainties for stations with positions determined by a combination of GPS and conventional surveying are larger and are dominated by the vertical uncertainty (uncertainty in height above the geoid). The method used to form the covariance matrix is described below.

The analysis of VLBI data from DSN antennas by Steppe et al. [7] includes a covariance matrix describing the uncertainty in the locations of the participating DSN antennas. The formal covariance probably is optimistic since there are usually some relevant parameters in any analysis that are imperfectly modeled. Boucher et al. [6], comparing the DSN VLBI station locations to other methods, find it necessary to scale the VLBI station location covariance by a factor of 2.25 to have the difference in station locations between various methods have the correct statistics. For forming a covariance for navigation teams, the formal covariance was multiplied by a factor of 4. This larger factor partially accounts for uncertainties in site velocities (plate motion); these uncertainties are separately accounted for by Boucher et al. [6] but cannot be separately accounted for within the ODP [10]. The coordinate uncertainties implied by the scaled VLBI covariance are 2 to 3 cm.

Besides scaling the formal VLBI covariance, an uncertainty in overall orientation was included to account for uncertainties between the station location reference frame and the terrestrial reference frame implied by delivered Earth orientation calibrations. In the most careful analysis comparing results from different space–geodetic techniques, it would appear possible to reduce this uncertainty to about 0.1 milliarcsecond (or 0.5 nrad, corresponding to about 0.3 cm at the surface of the Earth). However, the offsets between most measurement analyses, including JPL VLBI analysis, persist in showing offsets of order 1 milliarcsecond in spite of efforts to align reference frames [6]. For the station location covariance constructed here for navigation teams, an uncertainty of 1 milliarcsecond in rotation about each of three (x, y, and z) Earth-fixed axes has been folded in to account for this reference frame alignment uncertainty.

Stations that have not participated in DSN VLBI measurements have had their positions determined by either single short-baseline VLBI experiments or by a combination of GPS and conventional survey measurements. In the formation of this station location covariance, the uncertainty in the location of

[2] C. S. Jacobs and A. Rius, "Internal Consistency of VLBI Surveying Between DSS 63 and DSS 65," JPL Interoffice Memorandum 335.6-90-034 (internal document), Jet Propulsion Laboratory, Pasadena, California, May 11, 1992.

Table 4. Diagonal elements of the covariance matrix for the DSN station locations in cylindrical coordinates.

Station	Position method	Spin radius σ, m	Longitude σ, m	Z-height σ, m
DSS 12	DSN VLBI	0.03089	0.03925	0.03658
DSS 13	Short VLBI	0.04906	0.04490	0.04755
DSS 14	DSN VLBI	0.02287	0.03437	0.03039
DSS 15	DSN VLBI	0.02108	0.03340	0.02869
DSS 16	GPS survey	0.08711	0.04707	0.07057
DSS 17	GPS survey	0.08711	0.04707	0.07057
DSS 23	GPS survey	0.08653	0.04600	0.06986
DSS 24	GPS survey	0.08711	0.04707	0.07057
DSS 25	GPS survey	0.08711	0.04707	0.07057
DSS 26	GPS survey	0.08711	0.04707	0.07057
DSS 27	GPS survey	0.08711	0.04707	0.07057
DSS 28	GPS survey	0.08711	0.04707	0.07057
DSS 33	GPS survey	0.08770	0.04664	0.06990
DSS 34	GPS survey	0.08827	0.04770	0.07061
DSS 42	Short VLBI	0.04103	0.03897	0.03863
DSS 43	DSN VLBI	0.02906	0.03558	0.03099
DSS 45	DSN VLBI	0.02539	0.03428	0.02886
DSS 46	Survey	0.03232	0.03969	0.03511
DSS 53	GPS survey	0.08304	0.04672	0.07609
DSS 54	Pre-survey	4.02110	2.00032	3.58216
DSS 61	DSN VLBI	0.03410	0.03668	0.03803
DSS 63	DSN VLBI	0.02649	0.03531	0.03271
DSS 65	DSN VLBI	0.02494	0.03439	0.03103
DSS 66	GPS survey	0.08304	0.04672	0.07609

a surveyed antenna is the uncertainty in the location of the reference antenna augmented by additional uncertainty associated with the survey method. For antennas with positions determined by short-baseline VLBI experiments, the additional uncertainty used is the uncertainty given by the VLBI analyst; this is typically 1 to 2 cm in the north and east directions and 2 to 3 cm in the vertical. Most of the remaining antennas have had the position of a monument at the base of the antenna determined with respect to a GPS monument through a combination of GPS measurements and conventional surveying. The positions of the GPS monuments in turn were determined with respect to VLBI antennas through conventional surveys. The uncertainties of the antenna monument positions are assumed to be 2 cm in the north and east directions and 3 cm in the vertical. This is somewhat pessimistic for some of the monuments since conventional and GPS surveying are capable of sub-cm accuracy if carefully done. For most of the new antennas, the GPS part of the surveying was done with the goal of few-cm accuracy and so did not involve enough data collection to achieve sub-cm accuracy. The locations of the antennas above the monuments were inferred from construction drawings rather than direct measurements. The uncertainty in the vertical associated with this inference, therefore, is not strictly quantified. For the purposes of constructing a station location covariance for navigation teams, the uncertainty of the vertical component of these station locations increased by 10 cm.

One antenna, DSS 46, has had its position determined with respect to other antennas by conventional survey between the intersection of axes. This was carefully done and probably had an accuracy of 1 cm

or better. However, because there are offsets between the intersection of antenna axes and the effective station location of order 1 cm or more, due to antenna deformation caused by gravity, the relative uncertainty for this station was assumed to be 2 cm in the north, east, and vertical components with respect to the reference antenna (DSS 45).

In the past, navigation teams often have assumed that the uncertainty in station locations was large enough to cover uncertainties in Earth orientation. This is not the case for real-time data processing with the covariance described here. For processing radio metric data older than 2 weeks from the epoch of analysis (trajectory reconstruction), and using Earth orientation calibrations based on measurements later than the last tracking measurement, the uncertainty in Earth orientation is small compared to the station location uncertainties given below. For analysis of real-time data, the uncertainty in Earth orientation is larger than the station location uncertainty by a factor of 3 to 10, depending on the data incorporated into the Earth orientation calibration delivery. The ODP includes parameters that could be used to account for uncertainty in Earth orientation but does not have statistical models appropriate for modeling the random variations in Earth orientation. One possible approximation would be to estimate the Earth orientation parameters as Markov random processes with a several-day time constant and with an a priori uncertainty of 0.5 milliarcsecond (2.5 nrad) for times up until 2 weeks before the analysis epoch, and increasing to 10 milliarcsecond at the current epoch. Earth orientation uncertainty modeling, and its consequences, are described in more detail in [11].

V. Summary

The locations of the DSN tracking antennas have been determined with an accuracy of 15 cm (1σ) or better in order to satisfy present mission requirements for interplanetary navigation. Many antenna locations are known with 3-cm or better accuracy. The positions of all DSN antennas can be determined to 3-cm or better accuracy by combining the present survey information with additional measurements of antenna heights, if this is required by future mission navigation requirements.

Acknowledgments

Many people have been involved in collecting the information reflected in this station set. In particular, I would like to thank the following for direct assistance in the past year: Jim Richardson, Mike Heflin, Willy Bertiger, Brian Murphy, Ron van Hek, Alan Steppe, Jack Carper, Alan Robinson, Matthew Smith, Charles Black, Agustin Chamarro, Ted Moyer, Mark Ryne, and John Reynolds.

References

[1] J. O. Light, "An Investigation of the Orbit Redetermination Process Following the First Mid-Course Maneuver," *Supporting Research and Advanced Development, Space Programs Summary 37-33*, vol. IV, Jet Propulsion Laboratory, Pasadena, California, pp. 8–17, June 30, 1965.

[2] T. W. Hamilton and W. G. Melbourne, "Information Content of a Single Pass of Doppler Data From a Distant Spacecraft," *The Deep Space Network, Space Programs Summary 37-39*, vol. III, Jet Propulsion Laboratory, Pasadena, California, pp. 18–23, May 31, 1966.

[3] D. W. Curkendall and S. R. McReynolds, "A Simplified Approach for Determining the Information Content of Radio Tracking Data," *Journal of Spacecraft and Rockets*, vol. 6, no. 5, pp. 520–525, May 1969.

[4] O. J. Sovers, C. D. Edwards, C. S. Jacobs, G. E. Lanyi, K. M. Liewer, and R. N. Treuhaft, "Astrometric Results of 1978–1985 Deep Space Network Radio Interferometry; The JPL 1987-1 Extragalactic Radio Source Catalog," *Astr. J.*, vol. 95, pp. 1647–1658, 1988.

[5] C. Ma, J. W. Ryan, D. Gordan, D. S. Caprette, and W. E. Himwich, "Reference Frames From CDP VLBI Data," *Geodynamics*, vol. 24, pp. 121–145, 1993.

[6] C. Boucher, Z. Altamimi, M. Feissel, and P. Sillard, *Results and Analysis of the ITRF94*, IERS Technical Note 20, Observatoire de Paris, France, 1996.

[7] J. A. Steppe, S. H. Oliveau, and O. J. Sovers, "Earth Rotation Parameters From DSN VLBI: 1995," in P. Charlot, *Earth Orientation, Reference Frames, and Atmospheric Excitation Functions*, IERS Technical Note 19, in *1994 IERS Annual Report*, Observatoire de Paris, France, in press.

[8] C. Boucher, Z. Altamimi, and L. Duhem, *Results and Analysis of the ITRF93*, IERS Technical Note 18, Observatoire de Paris, France, October 1994.

[9] D. McCarthy, *IERS Standards*, IERS Technical Note 13, Observatoire de Paris, France, July 1992.

[10] T. Moyer, *Mathematical Formulation of the Double-Precision Orbit Determination Program*, JPL Technical Report 32-1527, Jet Propulsion Laboratory, Pasadena, California, 1971.

[11] J. A. Estefan and W. M. Folkner, "Sensitivity of Planetary Cruise Navigation to Earth Orientation Calibration Errors," *The Telecommunications and Data Acquisition Progress Report 42-123, July–September 1995*, Jet Propulsion Laboratory, Pasadena, California, pp. 1–29, November 15, 1995.
http://tda.jpl.nasa.gov/tda/progress_report/42-123/123E.pdf

[12] L. P. Teitelbaum, R. P. Linfield, G. M. Resch, S. J. Keihm, and M. J. Mahoney, "A Demonstration of Precise Calibration of Tropospheric Delay Fluctuations With Water Vapor Radiometers," *The Telecommunications and Data Acquisition Progress Report 42-126, April–June 1996*, Jet Propulsion Laboratory, Pasadena, California, pp. 1–8, August 15, 1996.
http://tda.jpl.nasa.gov/tda/progress_report/42-126/126H.pdf

Appendix A
Survey Information by Antenna

This appendix gives, for each DSN antenna, a description of the antenna reference points and the data used to determine its position. The high-efficiency (HEF) antennas at each site are used as reference antennas since they have participated in the most VLBI measurements. The HEF and the newer beam-waveguide (BWG) antennas have an azimuth/elevation (A-E) mount. Other antenna types include hour-angle/declination (H-D) mounts or west–east/north–south (X-Y) mounts. The 11-m antennas constructed for the orbiting VLBI missions (OVLBI) have azimuth/elevation mounts with a third axis adjustment for zenith-crossing tracks.

DSS 12, 34-m H-D Antenna

The reference point is the center of the hour-angle axis. Short-baseline VLBI experiments have been used to determine the position of DSS 12 relative to other antennas at the Goldstone complex. The short-baseline ties are reflected in interstation coordinates reported by Steppe et al. [7]. They give the following position vector:

Antennas	x, m	y, m	z, m
DSS 12–DSS 15	3094.978	−10331.330	−11039.0548

This has been added to the ITRF93 position for DSS 15.

DSS 13, 34-m BWG Antenna

The reference point is the intersection of the axes. The position of the new DSS 13 was determined with respect to DSS 15 from VLBI measurements by Teitelbaum et al. [12]. From their analysis, they derive the following vector:

Antennas	x, m	y, m	z, m
DSS 13–DSS 15	2426.299	−13881.207	−15757.256

This has been added to the ITRF93 position for DSS 15.

DSS 14, 70-m A-E Antenna

The reference point is the intersection of the axes. Short-baseline VLBI experiments have been used to determine the position of DSS 14 relative to other antennas at the Goldstone complex. The short-baseline ties are reflected in interstation coordinates reported by J. A. Steppe et al. [7]. They give the following position vector:

Antennas	x, m	y, m	z, m
DSS 14–DSS 15	−82.461	307.9652	382.3271

This has been added to the ITRF93 position for DSS 15.

DSS 15, 34-m HEF Antenna

The reference point is the intersection of the axes. The position for this antenna is listed in the ITRF93 system as follows:

Antenna	x, m	y, m	z, m
DSS 15	−2353538.790	−4641649.507	3676670.043

DSS 16, 26-m X-Y Antenna

The reference point is the center of the x-axis. The position of this antenna was established by a combination of GPS and conventional surveying.[3] The positions of the outside corners of two of the four support feet, at the bottom of the steel base plates, were determined with respect to GPS monuments. The position of the intersection of the antenna vertical centerline with the plane containing the bottom of the base plates was then inferred. The vector from this point to the Goldstone GPS monument (GOLD) was determined to be

Antennas	x, m	y, m	z, m
DSS 16cl–GOLD	−1144.194	−5392.525	−7596.995

The position of the GOLD in ITRF93 is given by

Antenna	x, m	y, m	z, m
GOLD	−2353614.131	−4641385.401	3676976.483

From the drawings of the antenna (Fig. A-1), the x-axis is 13.11 m above the bottom of the base plates. Combining the vertical correction with the differences of the ITRF93 coordinates of GOLD and DSS 15 gives the following position vector:

[3] J. Richardson, personal communication, Sterling Software, Boulder, Colorado, August 1994.

Antennas	x, m	y, m	z, m
DSS 16–DSS 15	−1224.368	−5137.955	−7282.974

This has been added to the ITRF93 position for DSS 15.

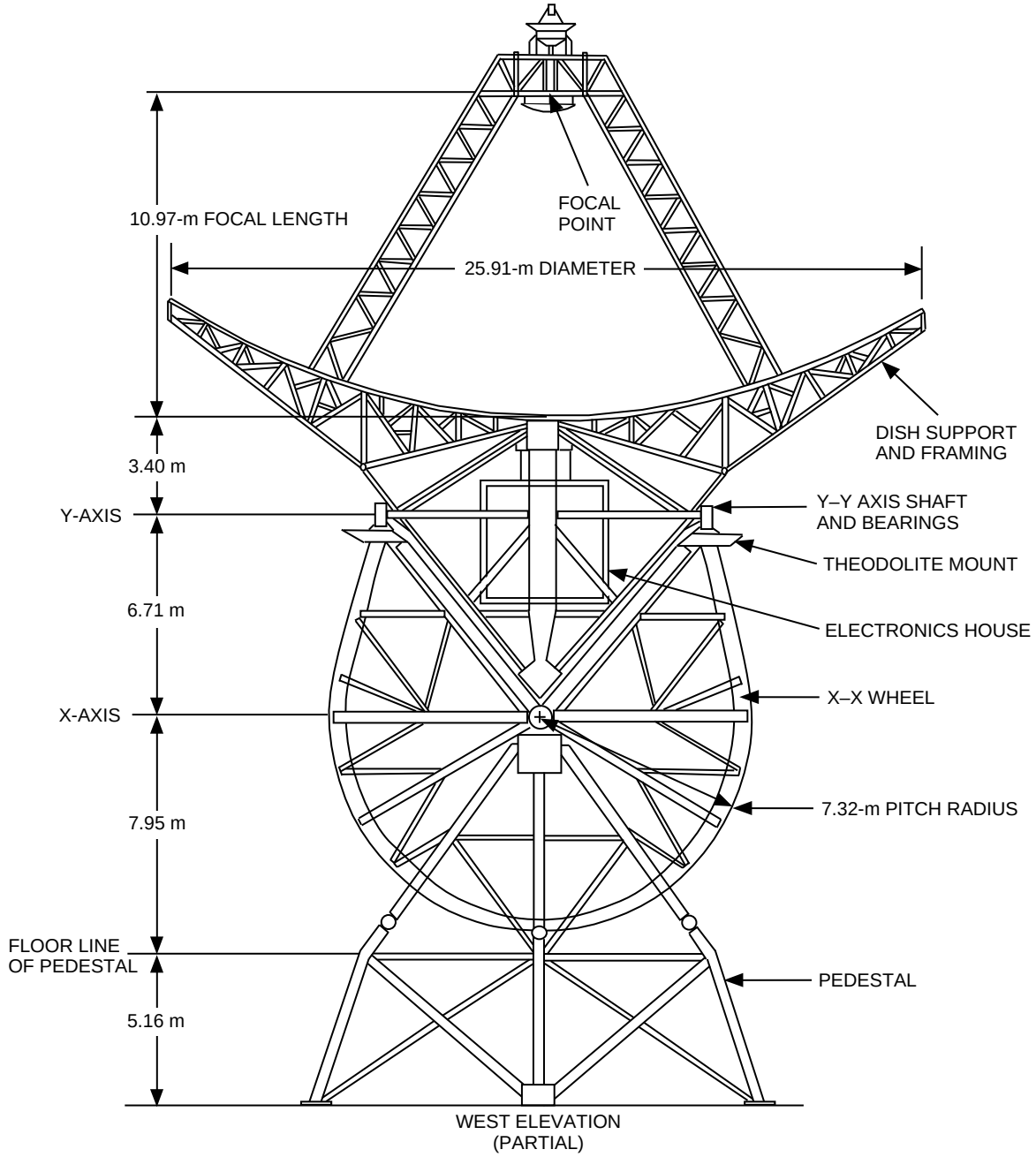

Fig. A-1. Drawing of a 26-m antenna (DSSs 16 and 66) showing a height of 13.11 m from the bottom of the steel feet (top of the concrete pillars) to the x-axis.

DSS 17, 9-m X-Y Antenna

The reference point is the center of the x-axis. The position of this antenna was established by a combination of GPS and conventional surveying.[4] The positions of the outside corners of two of the four support feet, at the bottom of the steel base plates, were determined with respect to GPS monuments. The position of the intersection of the antenna vertical centerline with the plane containing the bottom of the base plates was then inferred. The vector from this point to the Goldstone GPS monument, GOLD, was determined to be

Antennas	x, m	y, m	z, m
DSS 17cl–GOLD	−1113.997	−5361.976	−7539.321

From the drawings of the antenna (Fig. A-2), the x-axis is 6.04 m above the bottom of the base plates. Combining the vertical correction with the differences of the ITRF93 coordinates of GOLD and DSS 15 gives the following position vector:

Antennas	x, m	y, m	z, m
DSS 17–DSS 15	−1191.567	−5102.269	−7229.384

This has been added to the ITRF93 position for DSS 15.

DSS 23, 11-m OVLBI Antenna

The reference point is the center of motion of the elevation axis. The position of this antenna was established by a GPS survey.[5] The monument in the center of the concrete pad was occupied by a GPS receiver. The position was established with respect to the permanent Goldstone GPS monument, GOLD. The vector from the monument to GOLD was determined to be

Antennas	x, m	y, m	z, m
DSS 23m–GOLD	−1139.367	−5541.245	−7775.041

From the drawings of the antenna (Fig. A-3), the elevation axis is 11.04 m above the monument. Combining the vertical correction with the differences of the ITRF93 coordinates of GOLD and DSS 15 gives the following position vector:

Antennas	x, m	y, m	z, m
DSS 23–DSS 15	−1218.777	−5285.168	−7462.219

This has been added to the ITRF93 position for DSS 15.

[4] Ibid.

[5] Ibid.

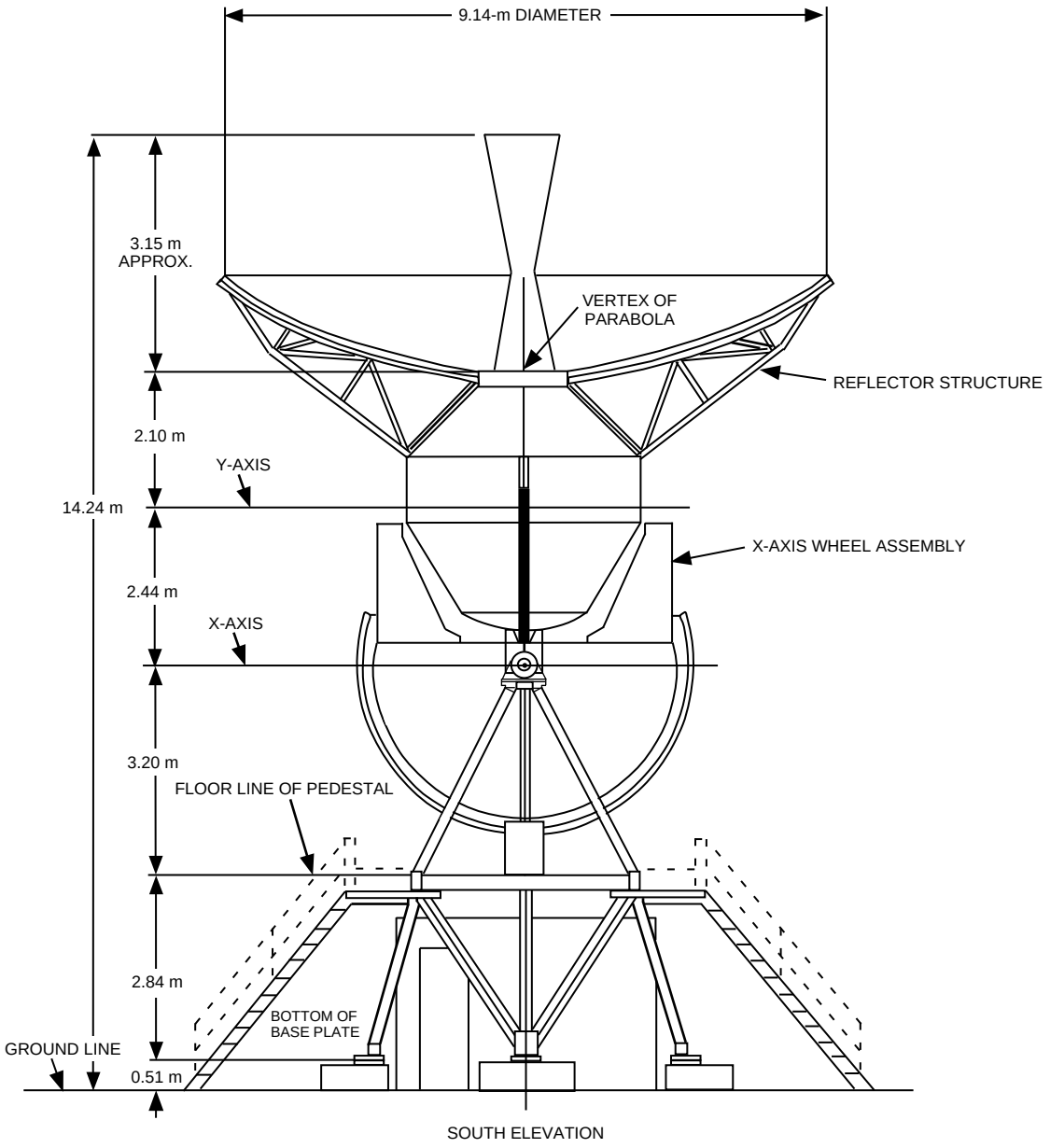

Fig. A-2. Drawing of a 9-m antenna (DSS 17) showing a height of 6.04 m from the bottom of the steel base plates to the x-axis.

DSS 24, 34-m BWG Antenna

The reference point is the intersection of the axes. The position of this antenna was established by a combination of GPS and conventional surveying.[6] The position of the monument in the center of the floor of the pedestal room was determined with respect to GPS monuments. The vector from this point to the Goldstone GPS monument, GOLD, was determined to be

[6] Ibid.

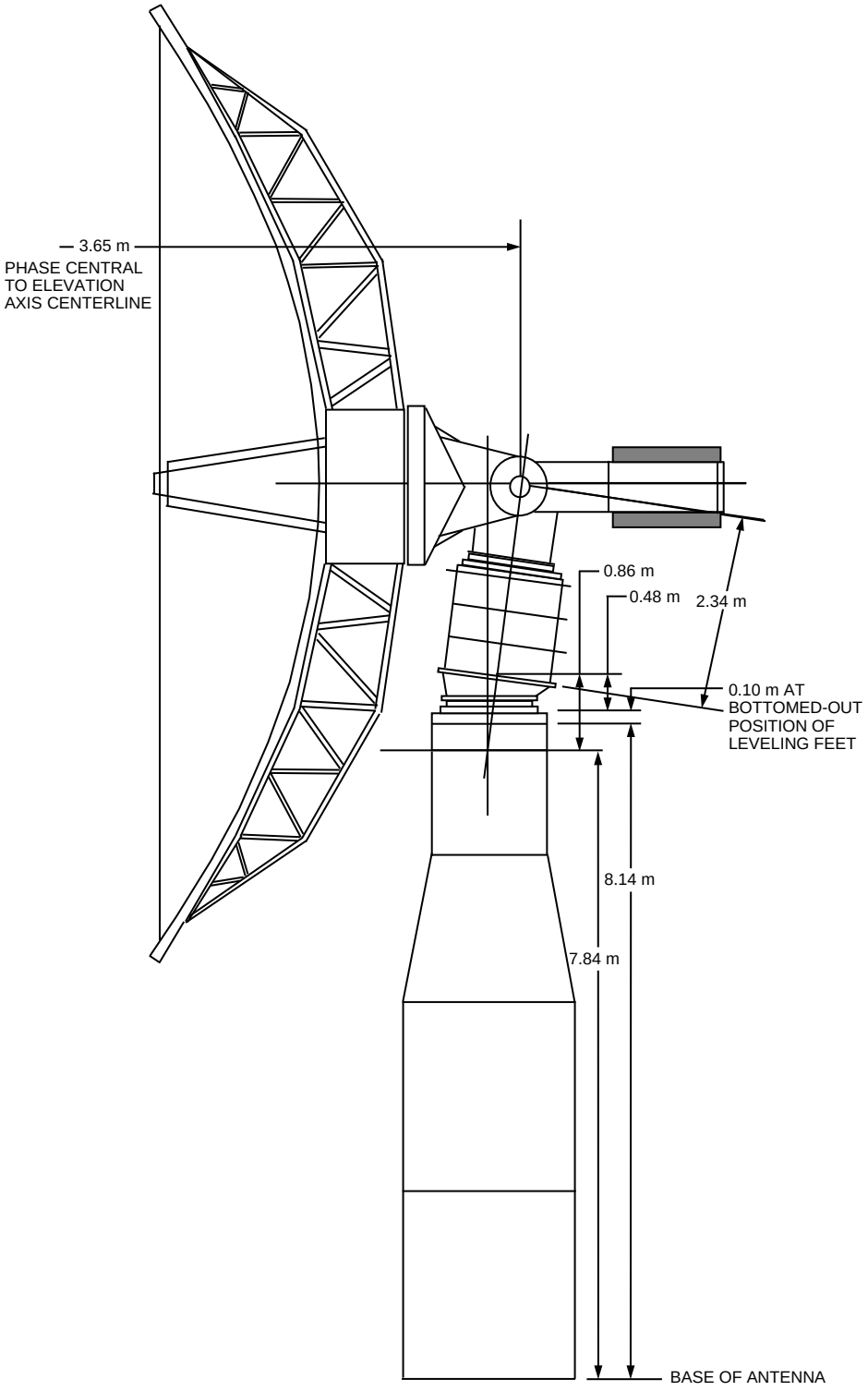

Fig. A-3. Sketch of an 11-m antenna (DSSs 23, 33, and 53) showing a height of 8.14 m + 0.10 m + 0.48 m + 2.34 m cos (7 deg) for the elevation axis above ground level. The finished height is expected to be higher when the azimuth axis is leveled.

Antennas	x, m	y, m	z, m
DSS 24m–GOLD	−1283.035	−5436.319	−7748.800

From the drawings of the antenna (Fig. A-4), the elevation axis is 25.30 m above the monument. Combining the vertical correction with the differences of the ITRF93 coordinates of GOLD and DSS 15 gives the following position vector:

Antennas	x, m	y, m	z, m
DSS 24–DSS 15	−1367.705	−5190.621	−7427.726

This has been added to the ITRF93 position for DSS 15.

DSS 25, 34-m BWG Antenna

The reference point is the intersection of the axes. The monument in the center of the pedestal room was surveyed with respect to several monuments at the Apollo site, with the following relative coordinates:[7]

Monument	East, m	North, m	Vertical, m
E1	712162.94	204849.97	000962.69
E2	712385.47	204849.97	000969.43
DSS 25	711915.40	204414.14	000964.23
DSS 23	712142.71	204629.25	000963.98

Positions for monuments E1 and E2 were determined by a GPS survey.[8] Their positions with respect to the permanent GPS monument, GOLD, are given by

Monuments	x, m	y, m	z, m
E1–GOLD	−1063.079	−5435.383	−7595.881
E2–GOLD	− 867.045	−5540.855	−7592.002

A rotation was estimated so that the rotated east–north–vertical vectors used by Carper would give the same relative positions for E1 and E2 as established by GPS. It was necessary to use the position of DSS 23 to solve for the rotation; the position for DSS 23 used by Carper was loosely weighted since the position predated construction. The estimated rotation was

[7] J. Carper, personal communication, Kenyon and Associates, Barstow, California, August 17, 1995.

[8] J. Richardson, op. cit.

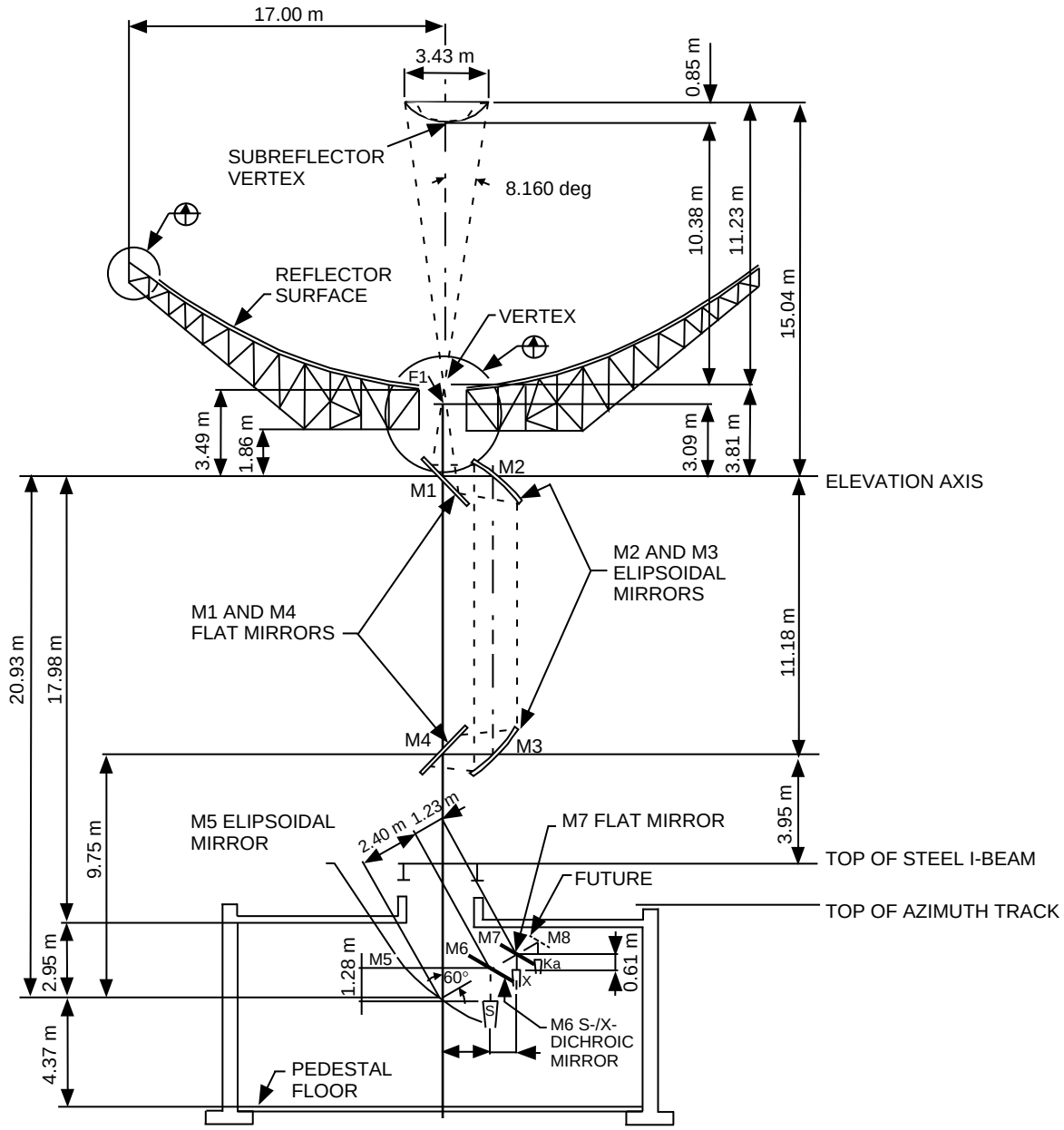

Fig. A-4. Drawing of a 34-m BWG antenna (DSSs 24, 25, 26, 34, and 54) showing a height of 25.30 m from the pedestal room floor (where the monument is located) to the elevation axis.

$$\begin{pmatrix} 0.892049 & 0.261874 & -0.368334 \\ -0.451938 & 0.516710 & -0.727161 \\ -0.000103 & 0.815128 & 0.579282 \end{pmatrix} \begin{pmatrix} e \\ n \\ v \end{pmatrix} = \begin{pmatrix} x \\ y \\ z \end{pmatrix}$$

After rotation, the E1–E2 vectors agree to about 1 cm. The rotated positions were used along with the GPS position of E1 to get the position vector:

Antennas	x, m	y, m	z, m
DSS 25m–GOLD	−1398.607	−5549.827	−7950.222

From the drawings of the antenna (Fig. A-4), the elevation axis is 25.30 m above the monument. Combining the vertical correction with the differences of the ITRF93 coordinates of GOLD and DSS 15 gives the following position vector:

Antennas	x, m	y, m	z, m
DSS 25–DSS 15	−1483.276	−5304.129	−7629.148

This has been added to the ITRF93 position for DSS 15.

DSS 26, 34-m BWG Antenna

The reference point is the intersection of the axes. The monument in the center of the pedestal room was surveyed in the same manner as was DSS 25. The following coordinates were supplied:[9]

Antenna	East, m	North, m	Vertical, m
DSS 26	712128.75	204200.76	973.33

This position minus the position of monument E1 was rotated using the same rotation matrix used for DSS 25 and combined with the GPS position of E1 to get the position vector with respect to the Goldstone GPS monument, GOLD:

Antennas	x, m	y, m	z, m
DSS 26m–GOLD	−1267.508	−5763.116	−8118.9052

From the drawings of the antenna (Fig. A-4), the elevation axis is 25.30 m above the monument. Combining the vertical correction with the differences of the ITRF93 coordinates of GOLD and DSS 15 gives the following position vector:

Antennas	x, m	y, m	z, m
DSS 26–DSS 15	−1352.177	−5517.418	−7797.831

This has been added to the ITRF93 position for DSS 15.

[9] J. Carper, op. cit.

DSS 27, 34-m A-E Antenna

The reference point is the center of the elevation axis. The position of this antenna was established by a combination of GPS and conventional surveying.[10] The position of the monument in the center of the floor of the pedestal room was determined with respect to GPS monuments. The vector from this point to the Goldstone GPS monument, GOLD, was determined to be

Antennas	x, m	y, m	z, m
DSS 27m–GOLD	3706.743	−15355.484	−16892.298

From the drawings of the antenna (Figs. A-5 and A-6), the elevation axis is 21.39 m above the monument. Combining the vertical correction with the differences of the ITRF93 coordinates of GOLD and DSS 15 gives the following position vector:

Antennas	x, m	y, m	z, m
DSS 27–DSS 15	3623.530	−15106.977	−16573.514

This has been added to the ITRF93 position for DSS 15.

DSS 28, 34-m A-E Antenna

The reference point is the center of the elevation axis. The position of this antenna was established by a combination of GPS and conventional surveying done by Jim Richardson in August 1994. The position of the monument in the center of the floor of the pedestal room was determined with respect to GPS monuments. The vector from this point to the Goldstone GPS monument, GOLD, was determined to be

Antennas	x, m	y, m	z, m
DSS 28m–GOLD	3520.1535	−15272.447	−16885.249

From the drawings of the antenna (Figs. A-5 and A-6), the elevation axis is 21.39 m above the monument. Combining the vertical correction with the differences of the ITRF93 coordinates of GOLD and DSS 15 gives the following position vector:

Antennas	x, m	y, m	z, m
DSS 27–DSS 15	3436.941	−15023.940	−16566.466

This has been added to the ITRF93 position for DSS 15.

[10] J. Richardson, op. cit.

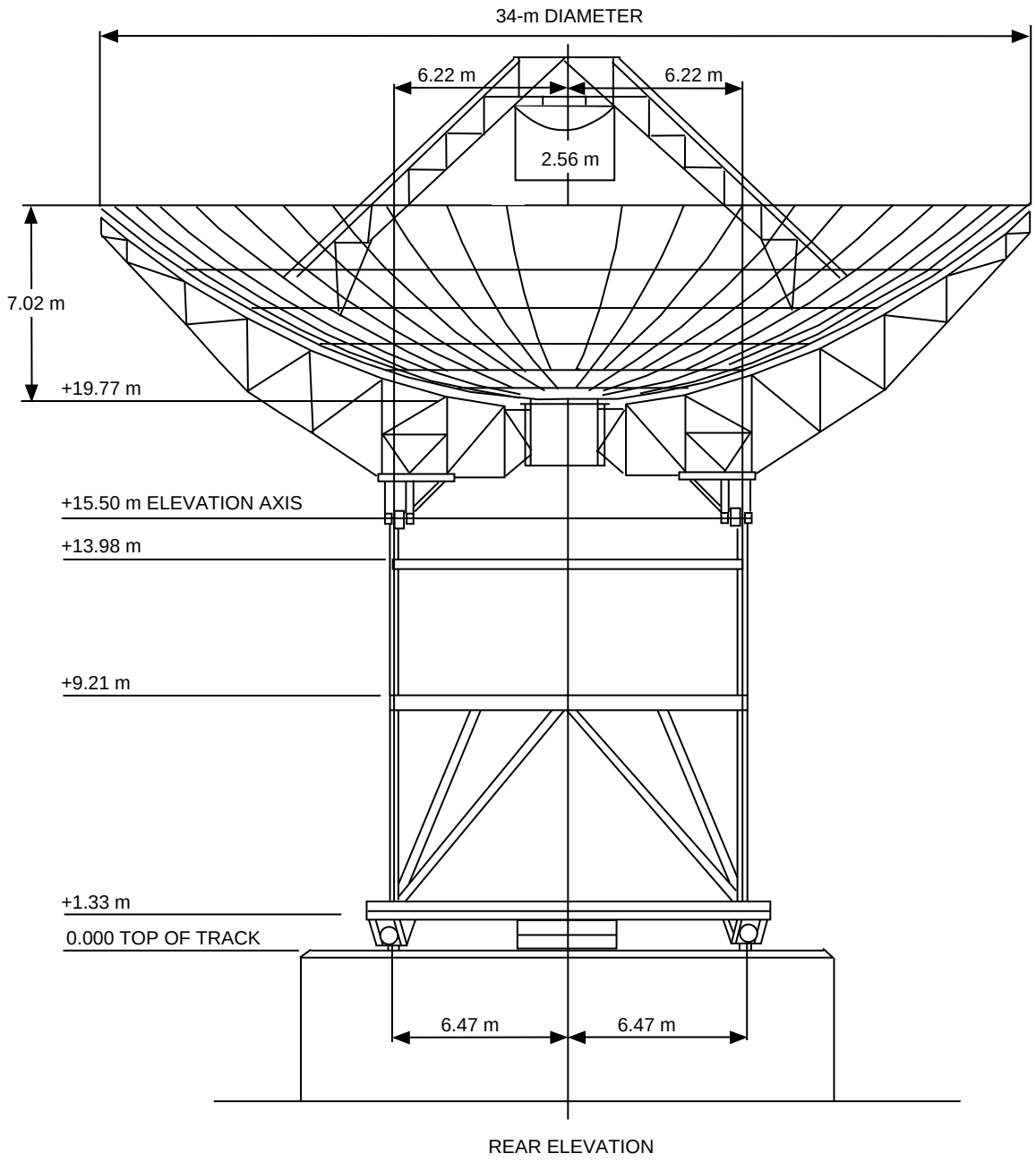

Fig. A-5. Drawing of the top of a 34-m A-E antenna (DSSs 27 and 28) showing a height of 15.50 m from the top of the track to the elevation axis.

DSS 33, 11-m OVLBI Antenna

The reference point is the center of motion of the elevation axis. The monument at the center of the concrete pad for DSS 33 was surveyed with respect to the Canberra GPS monument, TIDB, with the following coordinates:[11]

[11] B. Murphy, personal communication, Australian Surveying and Land Information Group, Belconnen, Australia, June 6, 1995.

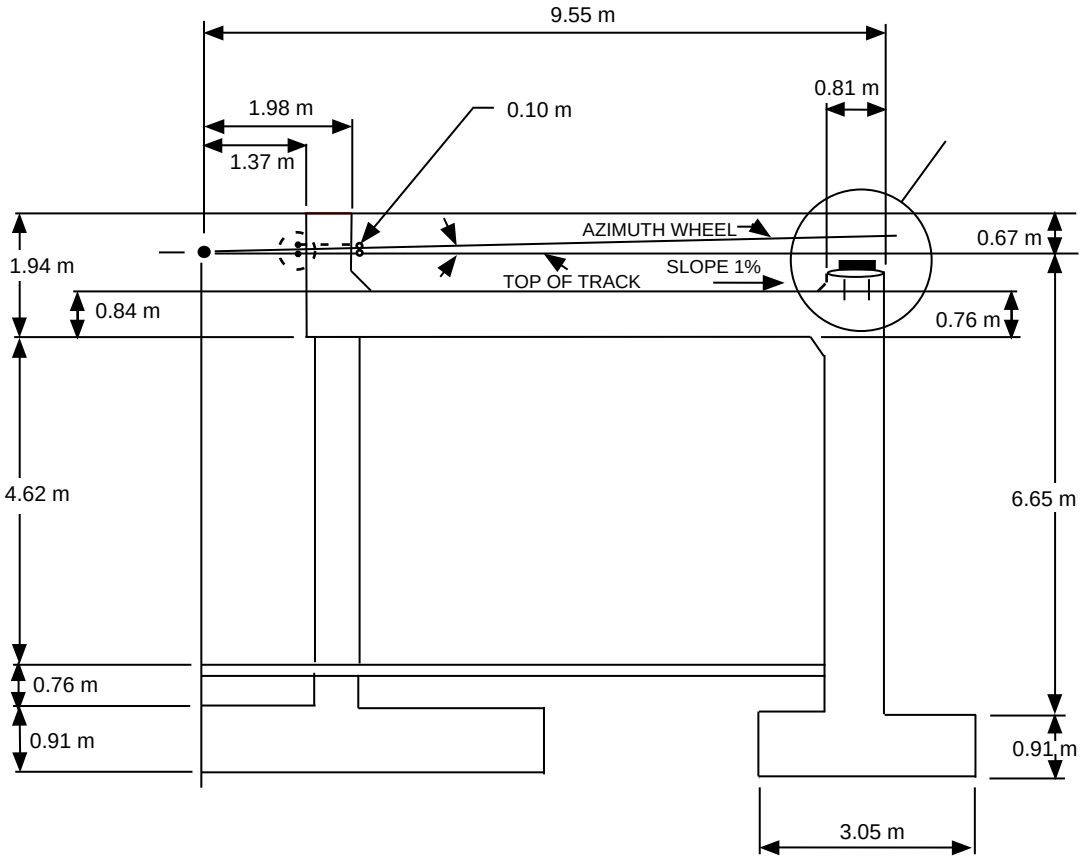

Fig A-6. Drawing of the bottom of a 34-m A-E antenna (DSSs 27 and 28) showing 5.89 m from the top of the pedestal room floor to the top of the track.

Monument	x, m	y, m	z, m
TIDB ITRF93	−4460995.999	2682557.108	−3674443.918
TIDB at 1995.2	−4460996.088	2682557.110	−3674443.810
DSS 33m at 1995.2	−4461075.895	2682277.112	−3674563.892

From the drawings of the antenna (Fig. A-3), the elevation axis is 11.034 m above the monument. Combining the vertical correction with the differences of the ITRF93 coordinates of TIDB and DSS 45 gives the following position vector:

Antennas	x, m	y, m	z, m
DSS 33–DSS 45	−148.264	−483.965	−188.990

This has been added to the ITRF93 position for DSS 45.

DSS 34, 34-m BWG Antenna

The reference point is the intersection of the axes. The position of the monument in the center of the floor of the pedestal room was determined with respect to the monument at the base of DSS 33, with the following coordinates:[12]

Antenna	Latitude			Longitude			Height, m
	deg	min	sec	deg	min	sec	
DSS 33m	S 35	24	1.760845	E 148	58	59.122234	673.073
DSS 34m	S 35	23	54.539371	E 148	58	55.063371	666.720

These have been converted from geodetic to Cartesian coordinates to get the position vector

Antennas	x, m	y, m	z, m
DSS 34m–DSS 33m	−53.278	151.557	185.113

From the drawing of the antenna (Fig. A-4), the elevation axis is 25.30 m above the monument. Combining the vertical correction with the differences of the ITRF93 coordinates of the DSS-33 monument and DSS 55 gives the following position vector:

Antennas	x, m	y, m	z, m
DSS 34–DSS 45m	−211.506	326.417	12.140

This has been added to the ITRF93 position for DSS 45.

DSS 42, 34-m H-D Antenna

The reference point is the center of the hour-angle axis. Short-baseline VLBI experiments have been used to determine the position of DSS 42 relative to other antennas at the Canberra complex. The short-baseline ties are reflected in interstation coordinates reported by J. A. Steppe et al. [7]. They give the following position vector:

Antennas	x, m	y, m	z, m
DSS 42–DSS 45	−45.766	−352.185	−200.670

This has been added to the ITRF93 position for DSS 45.

[12] B. Murphy, personal communication, Australian Surveying and Land Information Group, Belconnen, Australia, November 24, 1996.

DSS 43, 70-m A-E Antenna

The reference point is the intersection of the axes. Short-baseline VLBI experiments have been used to determine the position of DSS 43 relative to other antennas at the Goldstone complex. The short-baseline ties are reflected in interstation coordinates reported by J. A. Steppe et al. [7]. They give the following position vector:

Antennas	x, m	y, m	z, m
DSS 43–DSS 45	40.665	−404.156	−367.178

This has been added to the ITRF93 position for DSS 45.

DSS 45, 34-m HEF Antenna

The reference point is the intersection of the axes. The position for this antenna is listed in the ITRF93 system as

Antennas	x, m	y, m	z, m
DSS 45	−4460935.250	2682765.710	−3674381.402

DSS 46, 26-m X-Y Antenna

The reference point is the center of the x-axis. The position of this antenna was determined by a survey reported by Jim Steed, with the following position vector:[13]

Antennas	x, m	y, m	z, m
DSS 46–DSS 45	106.631	−636.154	−594.106

This has been added to the ITRF93 position for DSS 45.

Parkes, 64-m A-E Antenna

The reference point is the intersection of the axes. A short-baseline VLBI experiment was performed to determine the position of the Parkes 64-m antenna, giving the following position vector:[14]

[13] J. Steed, memorandum, Australian Surveying and Land Information Group, Belconnen, Australia, November 1, 1988.

[14] J. Reynolds, personal communication, Australia Telescope National Facility, Epping, New South Wales, Australia, April 10, 1994.

Antennas	x, m	y, m	z, m
Parkes–DSS 45	−93296.593	133993.273	220345.337

This has been added to the ITRF93 position of DSS 45.

DSS 53, 11-m OVLBI Antenna

The reference point is the center of motion of the elevation axis. The position of this antenna was established by a GPS survey.[15] The monument in the center of the concrete pad was occupied by a GPS receiver. The position was established with respect to the permanent Madrid GPS monument, MADR. The vector from the monument to MADR was determined to be

Antennas	x, m	y, m	z, m
DSS 53m–MADR	119.255	−8.276	−161.447

The position of the Madrid GPS receiver in ITRF93 is given by

Antenna	x, m	y, m	z, m
MADR	4849202.487	−0360329.192	4114913.049

From the drawings of the antenna (Fig. A-3), the elevation axis is 11.04 m above the monument. Combining the vertical correction with the differences of the ITRF93 coordinates of MADR and DSS 65 gives the following position vector:

Antennas	x, m	y, m	z, m
DSS 53–DSS 65	−6.612	150.769	9.983

This has been added to the ITRF93 position for DSS 65.

DSS 54, 34-m BWG Antenna

The reference point is the intersection of the axes. The position of this antenna is currently derived from positions printed on the Madrid site map. The coordinates used were

[15] J. Richardson, personal communication, Sterling Software, Boulder, Colorado, July 1995.

Antenna	East, m	North, m	Vertical, m
DSS 53m	394112.0	4476142.00	761.4
DSS 54g	393823.3	4475811.15	751.1

It was assumed that the center of the DSS-53 site is near the current monument and that the center of the DSS-54 site is the ground-level point. The differences in these coordinates were rotated using the rotation matrix

$$\begin{pmatrix} 0.0740739 & -0.64675 & 0.7590937 \\ 0.997252763 & 0.04803951 & -0.0563839 \\ 0 & 0.7611849 & 0.64853493 \end{pmatrix} \begin{pmatrix} e \\ n \\ v \end{pmatrix} = \begin{pmatrix} x \\ y \\ z \end{pmatrix}$$

to get the position vector

Antennas	x, m	y, m	z, m
DSS 54g–DSS 53m	184.800	−303.185	−258.498

According to a message from Gene Thom, the elevation axis is planned to be 17.7 m above ground level.[16] Adding this correction and the difference in coordinates of the OVLBI monument and DSS 65 gives the position vector

Antennas	x, m	y, m	z, m
DSS 54–DSS 65	183.248	−152.792	−244.192

This was added to the ITRF93 position of DSS 65.

DSS 61, 34-m H-D Antenna

The reference point is the center of the hour-angle axis. Short-baseline VLBI experiments have been used to determine the position of DSS 61 relative to other antennas at the Madrid complex. The short-baseline ties are reflected in interstation coordinates reported by J. A. Steppe et al. [7]. They give the following position vector:

Antennas	x, m	y, m	z, m
DSS 61–DSS 65	−91.520	210.694	135.670

This has been added to the ITRF93 position for DSS 65.

[16] G. Thom, personal communication, Jet Propulsion Laboratory, Pasadena, California, August 10, 1995.

DSS 63, 70-m A-E Antenna

The reference point is the intersection of the axes. Short-baseline VLBI experiments have been used to determine the position of DSS 63 relative to other antennas at the Madrid complex. The short-baseline ties are reflected in interstation coordinates reported by J. A. Steppe et al. [7]. They give the following position vector:

Antennas	x, m	y, m	z, m
DSS 63–DSS 65	−244.083	308.290	360.338

This has been added to the ITRF93 position for DSS 65.

DSS 65, 34-m HEF Antenna

The reference point is the intersection of the axes. The position for this antenna is listed in the ITRF93 system as

Antenna	x, m	y, m	z, m
DSS 65	4849336.730	−0360488.859	4114748.775

DSS 66, 26-m X-Y Antenna

The reference point is the center of the x-axis. The position of this antenna was established by a combination of GPS and conventional surveying.[17] The positions of the outside corners of two of the four support feet, at the top of the steel base plates, were determined with respect to GPS monuments. The position of the intersection of the antenna vertical centerline with the plane containing the top of the base plates was then inferred. The vector from this point to the Madrid GPS monument, MADR, was determined to be

Antennas	x, m	y, m	z, m
DSS 66cl–MADR	−63.854	−144.913	73.505

From the drawings of the antenna (Fig. A-1), the x-axis is 13.06 m above the top of the base plates. Combining the vertical correction with the differences of the ITRF93 coordinates of MADR and DSS 15 gives the following position vector:

[17] J. Richardson, July 1995, op. cit.

Antennas	x, m	y, m	z, m
DSS 66–DSS 65	−198.097	14.754	237.779

This has been added to the ITRF93 position for DSS 65.

Appendix B

Station Location Covariance

The covariance matrix for the station locations gives the uncertainties in the location coordinates and the correlations between them. The general element of the covariance matrix is given by

$$\sigma_{ij} = \left\langle (x_i - \overline{x}_i)^2 (x_j - \overline{x}_i)^2 \right\rangle$$

where σ_{ij} is the element of the covariance matrix, with i and j taking on values from 1 to the number of coordinates (3 times the number of stations); x_i is the true value of the station coordinate and $\overline{x}_i$ is the nominal value of the station coordinate; and $\langle x \rangle$ indicates the expectation value of x. The Orbit Determination Program expects the station location covariance to be expressed in cylindrical coordinates: the radial distance, ρ, from the Earth's spin axis; the station longitude, γ; and the distance, z (height above or below), from the equator. Table B-1 gives the element index for the station coordinates, and Table B-2 gives the covariance. Longitude uncertainties have been converted from radians to centimeters by multiplying by a spin radius of 5204.234 km at Goldstone, 5205.492 km at Canberra, and 4962.719 km at Madrid. Since the covariance is symmetric, only the upper triangular part is listed. The Parkes antenna is not included in the covariance matrix since it is used (by the DSN) primarily for telemetry arraying, not radio metric tracking. The uncertainties for DSS 54 are not included here since they are not well known prior to the station construction and final survey information.

Table B-1. Station coordinate element index for covariance matrix.

Station	Spin radius	Longitude	Z-height
DSS 12	1	2	3
DSS 13	4	5	6
DSS 14	7	8	9
DSS 15	10	11	12
DSS 16	13	14	15
DSS 17	16	17	18
DSS 23	19	20	21
DSS 24	22	23	24
DSS 25	25	26	27
DSS 26	28	29	30
DSS 27	31	32	33
DSS 28	34	35	36
DSS 33	37	38	39
DSS 34	40	41	42
DSS 42	43	44	45
DSS 43	46	47	48
DSS 45	49	50	51
DSS 46	52	53	54
DSS 53	55	56	57
DSS 61	58	59	60
DSS 63	61	62	63
DSS 65	64	65	66
DSS 66	67	68	69

Table B-2. Station location covariance elements in cm^2.

Cov(1,1) = −9.542									
Cov(1,2) = −1.460,	6.964								
Cov(1,3) = −2.190,	0.168,	13.383							
Cov(1,4) = −4.338,	0.157,	−4.729,	24.070						
Cov(1,5) = 0.306,	5.049,	−0.404,	0.343,	9.118					
Cov(1,6) = −4.699,	−0.169,	8.220,	2.892,	−0.175,	22.606				
Cov(1,7) = 4.803,	0.115,	−4.468,	4.265,	0.139,	−4.767,	5.231			
Cov(1,8) = 0.205,	5.090,	−0.415,	0.325,	5.041,	−0.405,	0.372,	5.342		
Cov(1,9) = −4.499,	−0.162,	8.398,	−4.816,	−0.193,	8.137,	−4.422,	−0.161,	9.237	
Cov(1,10) = 4.338,	0.157,	−4.729,	4.445,	0.155,	−4.665,	4.265,	0.147,	−4.816,	4.445
Cov(1,11) = 0.306, 5.046	5.049,	−0.404,	0.343,	5.047,	−0.388,	0.307,	5.040,	−0.427,	0.343,
Cov(1,12) = −4.699, −0.175,	−0.169, 8.231	8.220,	−4.665,	−0.175,	8.231,	−4.767,	−0.183,	8.137,	−4.665,
Cov(1,13) = 4.338, 0.155,	0.157, −4.665,	−4.729, 75.876	4.445,	0.155,	−4.665,	4.265,	0.147,	−4.816,	4.445,
Cov(1,14) = 0.306, 5.046,	5.049, −0.388,	−0.404, 0.343,	0.343, 10.020	5.047,	−0.388,	0.307,	5.040,	−0.427,	0.343,
Cov(1,15) = −4.699, −0.175,	−0.169, 8.231,	8.220, 38.315,	−4.665, −0.175,	−0.175, 49.801	8.231,	−4.767,	−0.183,	8.137,	−4.665,
Cov(1,16) = 4.338, 0.155,	0.157, −4.665,	−4.729, 6.445,	4.445, 0.155,	0.155, −4.665,	−4.665, 75.876	4.265,	0.147,	−4.816,	4.445,
Cov(1,17) = 0.306, 5.046,	5.049, −0.388,	−0.404, 0.343,	0.343, 5.950,	5.047, −0.388,	−0.388, 0.343,	0.307, 10.020	5.040,	−0.427,	0.343,
Cov(1,18) = −4.699, −0.175,	−0.169, 8.231,	8.220, −4.665,	−4.665, −0.175,	−0.175, 10.231,	8.231, 38.315,	−4.767, −0.175,	−0.183, 49.801	8.137,	−4.665,
Cov(1,19) = 4.338, 0.155,	0.157, −4.665,	−4.729, 5.445,	4.445, 0.155,	0.155, −4.665,	−4.665, 5.445,	4.265, 0.155,	0.147, −4.665,	−4.816, 74.876	4.445,
Cov(1,20) = 0.306, 5.046,	5.049, −0.388,	−0.404, 0.343,	0.343, 5.498,	5.047, −0.388,	−0.388, 0.343,	0.307, 5.498,	5.040, −0.388,	−0.427, 0.343,	0.343, 9.568
Cov(1,21) = −4.699, −0.175, 48.801	−0.169, 8.231,	8.220, −4.665,	−4.665, −0.175,	−0.175, 9.231,	8.231, −4.665,	−4.767, −0.175,	−0.183, 9.231,	8.137, 38.315,	−4.665, −0.175,

Table B-2 (cont'd).

Cov(1,22) =
4.338, 0.157, −4.729, 4.445, 0.155, −4.665, 4.265, 0.147, −4.816, 4.445,
0.155, −4.665, 6.445, 0.155, −4.665, 6.445, 0.155, −4.665, 5.445, 0.155,
−4.665, 75.876

Cov(1,23) =
0.306, 5.049, −0.404, 0.343, 5.047, −0.388, 0.307, 5.040, −0.427, 0.343,
5.046, −0.388, 0.343, 5.950, −0.388, 0.343, 5.950, −0.388, 0.343, 5.498,
−0.388, 0.343, 10.020

Cov(1,24) =
−4.699, −0.169, 8.220, −4.665, −0.175, 8.231, −4.767, −0.183, 8.137, −4.665,
−0.175, 8.231, −4.665, −0.175, 10.231, −4.665, −0.175, 10.231, −4.665, −0.175,
9.231, 38.315, −0.175, 49.801

Cov(1,25) =
4.338, 0.157, −4.729, 4.445, 0.155, −4.665, 4.265, 0.147, −4.816, 4.445,
0.155, −4.665, 6.445, 0.155, −4.665, 6.445, 0.155, −4.665, 5.445, 0.155,
−4.665, 6.445, 0.155, −4.665, 75.876

Cov(1,26) =
0.306, 5.049, −0.404, 0.343, 5.047, −0.388, 0.307, 5.040, −0.427, 0.343,
5.046, −0.388, 0.343, 5.950, −0.388, 0.343, 5.950, −0.388, 0.343, 5.498,
−0.388, 0.343, 5.950, −0.388, 0.343, 10.020

Cov(1,27) =
−4.699, −0.169, 8.220, −4.665, −0.175, 8.231, −4.767, −0.183, 8.137, −4.665,
−0.175, 8.231, −4.665, −0.175, 10.231, −4.665, −0.175, 10.231, −4.665, −0.175,
9.231, −4.665, −0.175, 10.231, 38.315, −0.175, 49.801

Cov(1,28) =
4.338, 0.157, −4.729, 4.445, 0.155, −4.665, 4.265, 0.147, −4.816, 4.445,
0.155, −4.665, 6.445, 0.155, −4.665, 6.445, 0.155, −4.665, 5.445, 0.155,
−4.665, 6.445, 0.155, −4.665, 6.445, 0.155, −4.665, 75.876

Cov(1,29) =
0.306, 5.049, −0.404, 0.343, 5.047, −0.388, 0.307, 5.040, −0.427, 0.343,
5.046, −0.388, 0.343, 5.950, −0.388, 0.343, 5.950, −0.388, 0.343, 5.498,
−0.388, 0.343, 5.950, −0.388, 0.343, 5.950, −0.388, 0.343, 10.020

Cov(1,30) =
−4.699, −0.169, 8.220, −4.665, −0.175, 8.231, −4.767, −0.183, 8.137, −4.665,
−0.175, 8.231, −4.665, −0.175, 10.231, −4.665, −0.175, 10.231, −4.665, −0.175,
9.231, −4.665, −0.175, 10.231, −4.665, −0.175, 10.231, 38.315, −0.175, 49.801

Cov(1,31) =
4.338, 0.157, −4.729, 4.445, 0.155, −4.665, 4.265, 0.147, −4.816, 4.445,
0.155, −4.665, 5.445, 0.155, −4.665, 5.445, 0.155, −4.665, 5.445, 0.155,
−4.665, 5.445, 0.155, −4.665, 5.445, 0.155, −4.665, 5.445, 0.155, −4.665,
75.876

Cov(1,32) =
0.306, 5.049, −0.404, 0.343, 5.047, −0.388, 0.307, 5.040, −0.427, 0.343,
5.046, −0.388, 0.343, 5.498, −0.388, 0.343, 5.498, −0.388, 0.343, 5.498,
−0.388, 0.343, 5.498, −0.388, 0.343, 5.498, −0.388, 0.343, 5.498, −0.388,
0.343, 10.020

Cov(1,33) =
−4.699, −0.169, 8.220, −4.665, −0.175, 8.231, −4.767, −0.183, 8.137, −4.665,
−0.175, 8.231, −4.665, −0.175, 9.231, −4.665, −0.175, 9.231, −4.665, −0.175,
9.231, −4.665, −0.175, 9.231, −4.665, −0.175, 9.231, −4.665, −0.175, 9.231,
38.315, −0.175, 49.801

Cov(1,34) =
4.338, 0.157, −4.729, 4.445, 0.155, −4.665, 4.265, 0.147, −4.816, 4.445,
0.155, −4.665, 5.445, 0.155, −4.665, 5.445, 0.155, −4.665, 5.445, 0.155,
−4.665, 5.445, 0.155, −4.665, 5.445, 0.155, −4.665, 5.445, 0.155, −4.665,
6.445, 0.155, −4.665, 75.876

Table B-2 (cont'd).

Cov(1,35) =
0.306, 5.049, −0.404, 0.343, 5.047, −0.388, 0.307, 5.040, −0.427, 0.343,
5.046, −0.388, 0.343, 5.498, −0.388, 0.343, 5.498, −0.388, 0.343, 5.498,
−0.388, 0.343, 5.498, −0.388, 0.343, 5.498, −0.388, 0.343, 5.498, −0.388,
0.343, 5.950, −0.388, 0.343, 10.020

Cov(1,36) =
−4.699, −0.169, 8.220, −4.665, −0.175, 8.231, −4.767, −0.183, 8.137, −4.665,
−0.175, 8.231, −4.665, −0.175, 9.231, −4.665, −0.175, 9.231, −4.665, −0.175,
9.231, −4.665, −0.175, 9.231, −4.665, −0.175, 9.231, −4.665, −0.175, 9.231,
−4.665, −0.175, 10.231, 38.315, −0.175, 49.801

Cov(1,37) =
−0.134, 1.545, −0.488, −0.305, 1.548, −0.591, −0.085, 1.556, −0.416, −0.305,
1.547, −0.591, −0.305, 1.547, −0.591, −0.305, 1.547, −0.591, −0.305, 1.547,
−0.591, −0.305, 1.547, −0.591, −0.305, 1.547, −0.591, −0.305, 1.547, −0.591,
−0.305, 1.547, −0.591, −0.305, 1.547, −0.591, 76.913

Cov(1,38) =
−3.621, 3.072, 4.915, −3.748, 3.073, 4.836, −3.561, 3.084, 4.995, −3.748,
3.073, 4.836, −3.748, 3.073, 4.836, −3.748, 3.073, 4.836, −3.748, 3.073,
4.836, −3.748, 3.073, 4.836, −3.748, 3.073, 4.836, −3.748, 3.073, 4.836,
−3.748, 3.073, 4.836, −3.748, 3.073, 4.836, 1.038, 18.640

Cov(1,39) =
0.672, 2.210, −0.651, 0.758, 2.222, −0.583, 0.658, 2.219, −0.657, 0.758,
2.221, −0.583, 0.758, 2.221, −0.583, 0.758, 2.221, −0.583, 0.758, 2.221,
−0.583, 0.758, 2.221, −0.583, 0.758, 2.221, −0.583, 0.758, 2.221, −0.583,
0.758, 2.221, −0.583, 0.758, 2.221, −0.583, −38.962, −0.574, 48.862

Cov(1,40) =
−0.134, 1.545, −0.488, −0.305, 1.548, −0.591, −0.085, 1.556, −0.416, −0.305,
1.547, −0.591, −0.305, 1.547, −0.591, −0.305, 1.547, −0.591, −0.305, 1.547,
−0.591, −0.305, 1.547, −0.591, −0.305, 1.547, −0.591, −0.305, 1.547, −0.591,
−0.305, 1.547, −0.591, −0.305, 1.547, −0.591, 76.913, 0.890, −38.962, 77.913

Cov(1,41) =
−3.621, 3.072, 4.915, −3.748, 3.073, 4.836, −3.561, 3.084, 4.995, −3.748,
3.073, 4.836, −3.748, 3.073, 4.836, −3.748, 3.073, 4.836, −3.748, 3.073,
4.836, −3.748, 3.073, 4.836, −3.748, 3.073, 4.836, −3.748, 3.073, 4.836,
−3.748, 3.073, 4.836, −3.748, 3.073, 4.836, 1.038, 18.640, −0.669, 1.038,
19.497

Cov(1,42) =
0.672, 2.210, −0.651, 0.758, 2.222, −0.583, 0.658, 2.219, −0.657, 0.758,
2.221, −0.583, 0.758, 2.221, −0.583, 0.758, 2.221, −0.583, 0.758, 2.221,
−0.583, 0.758, 2.221, −0.583, 0.758, 2.221, −0.583, 0.758, 2.221, −0.583,
0.758, 2.221, −0.583, 0.758, 2.221, −0.583, −38.962, −0.574, 48.862, −38.962,
−0.574, 49.862

Cov(1,43) =
−0.301, 1.524, −0.691, −0.179, 1.536, −0.593, −0.531, 1.426, −1.082, −0.179,
1.536, −0.593, −0.179, 1.536, −0.593, −0.179, 1.536, −0.593, −0.179, 1.536,
−0.593, −0.179, 1.536, −0.593, −0.179, 1.536, −0.593, −0.179, 1.536, −0.593,
−0.179, 1.536, −0.593, −0.179, 1.536, −0.593, 6.082, 0.739, 4.221, 6.082,
0.739, 4.221, 16.831

Cov(1,44) =
−3.576, 3.074, 4.943, −3.719, 3.077, 4.854, −3.477, 3.097, 5.073, −3.719,
3.077, 4.854, −3.719, 3.077, 4.854, −3.719, 3.077, 4.854, −3.719, 3.077,
4.854, −3.719, 3.077, 4.854, −3.719, 3.077, 4.854, −3.719, 3.077, 4.854,
−3.719, 3.077, 4.854, −3.719, 3.077, 4.854, 1.002, 10.042, −0.654, 1.002,
10.042, −0.654, 1.251, 13.015

Table B-2 (cont'd).

Cov(1,45) =
0.810, 2.226, −0.494, 0.677, 2.231, −0.574, 1.016, 2.319, −0.140, 0.677,
2.231, −0.574, 0.677, 2.231, −0.574, 0.677, 2.231, −0.574, 0.677, 2.231,
−0.574, 0.677, 2.231, −0.574, 0.677, 2.231, −0.574, 0.677, 2.231, −0.574,
0.677, 2.231, −0.574, 0.677, 2.231, −0.574, 4.257, −0.475, 8.178, 4.257,
−0.475, 8.178, −0.568, −0.751, 14.926

Cov(1,46) =
−0.347, 1.508, −0.742, −0.189, 1.535, −0.601, −0.520, 1.430, −1.064, −0.189,
1.534, −0.601, −0.189, 1.534, −0.601, −0.189, 1.534, −0.601, −0.189, 1.534,
−0.601, −0.189, 1.534, −0.601, −0.189, 1.534, −0.601, −0.189, 1.534, −0.601,
−0.189, 1.534, −0.601, −0.189, 1.534, −0.601, 6.086, 0.746, 4.222, 6.086,
0.746, 4.222, 8.398, 0.960, 3.484, 8.443

Cov(1,47) =
−3.565, 3.077, 4.954, −3.720, 3.077, 4.855, −3.481, 3.096, 5.069, −3.720,
3.077, 4.855, −3.720, 3.077, 4.855, −3.720, 3.077, 4.855, −3.720, 3.077,
4.855, −3.720, 3.077, 4.855, −3.720, 3.077, 4.855, −3.720, 3.077, 4.855,
−3.720, 3.077, 4.855, −3.720, 3.077, 4.855, 1.005, 10.044, −0.656, 1.005,
10.044, −0.656, 1.113, 10.846, −0.761, 1.118, 10.848

Cov(1,48) =
0.849, 2.238, −0.451, 0.684, 2.232, −0.568, 1.007, 2.315, −0.156, 0.684,
2.232, −0.568, 0.684, 2.232, −0.568, 0.684, 2.232, −0.568, 0.684, 2.232,
−0.568, 0.684, 2.232, −0.568, 0.684, 2.232, −0.568, 0.684, 2.232, −0.568,
0.684, 2.232, −0.568, 0.684, 2.232, −0.568, 4.256, −0.480, 8.177, 4.256,
−0.480, 8.177, 3.480, −0.657, 9.580, 3.449, −0.654, 9.605

Cov(1,49) =
−0.134, 1.545, −0.488, −0.305, 1.548, −0.591, −0.085, 1.556, −0.416, −0.305,
1.547, −0.591, −0.305, 1.547, −0.591, −0.305, 1.547, −0.591, −0.305, 1.547,
−0.591, −0.305, 1.547, −0.591, −0.305, 1.547, −0.591, −0.305, 1.547, −0.591,
−0.305, 1.547, −0.591, −0.305, 1.547, −0.591, 6.447, 0.890, 4.006, 6.447,
0.890, 4.006, 6.082, 0.858, 4.257, 6.086, 0.861, 4.256, 6.447

Cov(1,50) =
−3.621, 3.072, 4.915, −3.748, 3.073, 4.836, −3.561, 3.084, 4.995, −3.748,
3.073, 4.836, −3.748, 3.073, 4.836, −3.748, 3.073, 4.836, −3.748, 3.073,
4.836, −3.748, 3.073, 4.836, −3.748, 3.073, 4.836, −3.748, 3.073, 4.836,
−3.748, 3.073, 4.836, −3.748, 3.073, 4.836, 1.038, 10.070, −0.669, 1.038,
10.070, −0.669, 0.863, 10.042, −0.555, 0.871, 10.044, −0.560, 1.038, 10.070

Cov(1,51) =
0.672, 2.210, −0.651, 0.758, 2.222, −0.583, 0.658, 2.219, −0.657, 0.758,
2.221, −0.583, 0.758, 2.221, −0.583, 0.758, 2.221, −0.583, 0.758, 2.221,
−0.583, 0.758, 2.221, −0.583, 0.758, 2.221, −0.583, 0.758, 2.221, −0.583,
0.758, 2.221, −0.583, 0.758, 2.221, −0.583, 4.006, −0.574, 8.328, 4.006,
−0.574, 8.328, 4.221, −0.560, 8.178, 4.222, −0.562, 8.177, 4.006, −0.574,
8.328

Cov(1,52) =
−0.134, 1.545, −0.488, −0.305, 1.548, −0.591, −0.085, 1.556, −0.416, −0.305,
1.547, −0.591, −0.305, 1.547, −0.591, −0.305, 1.547, −0.591, −0.305, 1.547,
−0.591, −0.305, 1.547, −0.591, −0.305, 1.547, −0.591, −0.305, 1.547, −0.591,
−0.305, 1.547, −0.591, −0.305, 1.547, −0.591, 6.447, 0.890, 4.006, 6.447,
0.890, 4.006, 6.082, 0.858, 4.257, 6.086, 0.861, 4.256, 6.447, 0.890,
4.006, 10.447

Cov(1,53) =
−3.621, 3.072, 4.915, −3.748, 3.073, 4.836, −3.561, 3.084, 4.995, −3.748,
3.073, 4.836, −3.748, 3.073, 4.836, −3.748, 3.073, 4.836, −3.748, 3.073,
4.836, −3.748, 3.073, 4.836, −3.748, 3.073, 4.836, −3.748, 3.073, 4.836,
−3.748, 3.073, 4.836, −3.748, 3.073, 4.836, 1.038, 10.070, −0.669, 1.038,
10.070, −0.669, 0.863, 10.042, −0.555, 0.871, 10.044, −0.560, 1.038, 10.070,
−0.669, 1.038, 13.498

Table B-2 (cont'd).

Cov(1,54) =
0.672, 2.210, −0.651, 0.758, 2.222, −0.583, 0.658, 2.219, −0.657, 0.758,
2.221, −0.583, 0.758, 2.221, −0.583, 0.758, 2.221, −0.583, 0.758, 2.221,
−0.583, 0.758, 2.221, −0.583, 0.758, 2.221, −0.583, 0.758, 2.221, −0.583,
0.758, 2.221, −0.583, 0.758, 2.221, −0.583, 4.006, −0.574, 8.328, 4.006,
−0.574, 8.328, 4.221, −0.560, 8.178, 4.222, −0.562, 8.177, 4.006, −0.574,
8.328, 4.006, −0.574, 12.328

Cov(1,55) =
−2.170, 1.515, 2.277, −2.341, 1.524, 2.184, −2.131, 1.538, 2.363, −2.341,
1.524, 2.184, −2.341, 1.524, 2.184, −2.341, 1.524, 2.184, −2.341, 1.524,
2.184, −2.341, 1.524, 2.184, −2.341, 1.524, 2.184, −2.341, 1.524, 2.184,
−2.341, 1.524, 2.184, −2.341, 1.524, 2.184, 4.736, 2.189, 3.840, 4.736,
2.189, 3.840, 4.474, 2.156, 4.016, 4.481, 2.159, 4.012, 4.736, 2.189,
3.840, 4.736, 2.189, 3.840, 68.954

Cov(1,56) =
−3.220, 2.398, 4.478, −3.112, 2.395, 4.537, −3.273, 2.388, 4.408, −3.112,
2.394, 4.537, −3.112, 2.394, 4.537, −3.112, 2.394, 4.537, −3.112, 2.394,
4.537, −3.112, 2.394, 4.537, −3.112, 2.394, 4.537, −3.112, 2.394, 4.537,
−3.112, 2.394, 4.537, −3.112, 2.394, 4.537, −2.601, 7.610, −1.699, −2.601,
7.610, −1.699, −2.389, 7.632, −1.844, −2.394, 7.630, −1.841, −2.601, 7.610,
−1.699, −2.601, 7.610, −1.699, −1.269, 21.764

Cov(1,57) =
1.391, −1.679, −2.765, 1.191, −1.685, −2.897, 1.472, −1.671, −2.666, 1.191,
−1.685, −2.897, 1.191, −1.685, −2.897, 1.191, −1.685, −2.897, 1.191, −1.685,
−2.897, 1.191, −1.685, −2.897, 1.191, −1.685, −2.897, 1.191, −1.685, −2.897,
1.191, −1.685, −2.897, 1.191, −1.685, −2.897, −1.921, −0.892, −6.582, −1.921,
−0.892, −6.582, −2.298, −0.933, −6.326, −2.290, −0.930, −6.331, −1.921, −0.892,
−6.582, −1.921, −0.892, −6.582, 41.350, −0.864, 57.894

Cov(1,58) =
−2.426, 1.569, 2.144, −2.188, 1.543, 2.259, −2.595, 1.725, 2.159, −2.188,
1.542, 2.259, −2.188, 1.542, 2.259, −2.188, 1.542, 2.259, −2.188, 1.542,
2.259, −2.188, 1.542, 2.259, −2.188, 1.542, 2.259, −2.188, 1.542, 2.259,
−2.188, 1.542, 2.259, −2.188, 1.542, 2.259, 4.419, 2.003, 3.999, 4.419,
2.003, 3.999, 4.326, 1.945, 4.040, 4.347, 1.955, 4.029, 4.419, 2.003,
3.999, 4.419, 2.003, 3.999, 5.923, −1.077, −3.946, 11.625

Cov(1,59) =
−3.368, 2.400, 4.409, −3.161, 2.393, 4.520, −3.560, 2.333, 4.409, −3.161,
2.392, 4.520, −3.161, 2.392, 4.520, −3.161, 2.392, 4.520, −3.161, 2.392,
4.520, −3.161, 2.392, 4.520, −3.161, 2.392, 4.520, −3.161, 2.392, 4.520,
−3.161, 2.392, 4.520, −3.161, 2.392, 4.520, −2.504, 7.662, −1.751, −2.504,
7.662, −1.751, −2.193, 7.675, −1.971, −2.204, 7.673, −1.964, −2.504, 7.662,
−1.751, −2.504, 7.662, −1.751, −1.188, 11.730, −0.756, −1.401, 13.419

Cov(1,60) =
1.320, −1.640, −2.803, 1.369, −1.667, −2.813, 1.196, −1.610, −2.536, 1.369,
−1.667, −2.813, 1.369, −1.667, −2.813, 1.369, −1.667, −2.813, 1.369, −1.667,
−2.813, 1.369, −1.667, −2.813, 1.369, −1.667, −2.813, 1.369, −1.667, −2.813,
1.369, −1.667, −2.813, 1.369, −1.667, −2.813, −2.270, −1.097, −6.406, −2.270,
−1.097, −6.406, −2.573, −1.152, −6.211, −2.549, −1.143, −6.224, −2.270, −1.097,
−6.406, −2.270, −1.097, −6.406, −3.893, −0.651, 9.214, −0.155, −0.969, 14.466

Cov(1,61) =
−2.543, 1.590, 2.102, −2.198, 1.543, 2.254, −2.565, 1.719, 2.166, −2.198,
1.543, 2.254, −2.198, 1.543, 2.254, −2.198, 1.543, 2.254, −2.198, 1.543,
2.254, −2.198, 1.543, 2.254, −2.198, 1.543, 2.254, −2.198, 1.543, 2.254,
−2.198, 1.543, 2.254, −2.198, 1.543, 2.254, 4.421, 2.006, 3.999, 4.421,
2.006, 3.999, 4.338, 1.957, 4.037, 4.340, 1.960, 4.036, 4.421, 2.006,
3.999, 4.421, 2.006, 3.999, 5.923, −1.083, −3.942, 7.001, −1.288, −3.341,
7.016

Table B-2 (cont'd).

Cov(1,62) =

−3.382, 2.402, 4.404, −3.162, 2.393, 4.521, −3.556, 2.332, 4.411, −3.162,
2.392, 4.521, −3.162, 2.392, 4.521, −3.162, 2.392, 4.521, −3.162, 2.392,
4.521, −3.162, 2.392, 4.521, −3.162, 2.392, 4.521, −3.162, 2.392, 4.521,
−3.162, 2.392, 4.521, −3.162, 2.392, 4.521, −2.505, 7.661, −1.751, −2.505,
7.661, −1.751, −2.200, 7.674, −1.967, −2.208, 7.673, −1.962, −2.505, 7.661,
−1.751, −2.505, 7.661, −1.751, −1.189, 11.731, −0.758, −1.288, 12.436, −0.890,
−1.292, 12.436

Cov(1,63) =

1.237, −1.624, −2.832, 1.361, −1.667, −2.817, 1.216, −1.615, −2.533, 1.361,
−1.666, −2.817, 1.361, −1.666, −2.817, 1.361, −1.666, −2.817, 1.361, −1.666,
−2.817, 1.361, −1.666, −2.817, 1.361, −1.666, −2.817, 1.361, −1.666, −2.817,
1.361, −1.666, −2.817, 1.361, −1.666, −2.817, −2.266, −1.093, −6.407, −2.266,
−1.093, −6.407, −2.558, −1.140, −6.217, −2.552, −1.138, −6.220, −2.266, −1.093,
−6.407, −2.266, −1.093, −6.407, −3.891, −0.656, 9.219, −3.344, −0.891, 10.687,
−3.329, −0.892, 10.700

Cov(1,64) =

−2.170, 1.515, 2.277, −2.341, 1.524, 2.184, −2.131, 1.538, 2.363, −2.341,
1.524, 2.184, −2.341, 1.524, 2.184, −2.341, 1.524, 2.184, −2.341, 1.524,
2.184, −2.341, 1.524, 2.184, −2.341, 1.524, 2.184, −2.341, 1.524, 2.184,
−2.341, 1.524, 2.184, −2.341, 1.524, 2.184, 4.736, 2.189, 3.840, 4.736,
2.189, 3.840, 4.474, 2.156, 4.016, 4.481, 2.159, 4.012, 4.736, 2.189,
3.840, 4.736, 2.189, 3.840, 6.222, −1.265, −3.571, 5.923, −1.184, −3.893,
5.923, −1.186, −3.891, 6.222

Cov(1,65) =

−3.220, 2.398, 4.478, −3.112, 2.395, 4.537, −3.273, 2.388, 4.408, −3.112,
2.394, 4.537, −3.112, 2.394, 4.537, −3.112, 2.394, 4.537, −3.112, 2.394,
4.537, −3.112, 2.394, 4.537, −3.112, 2.394, 4.537, −3.112, 2.394, 4.537,
−3.112, 2.394, 4.537, −3.112, 2.394, 4.537, −2.601, 7.610, −1.699, −2.601,
7.610, −1.699, −2.389, 7.632, −1.844, −2.394, 7.630, −1.841, −2.601, 7.610,
−1.699, −2.601, 7.610, −1.699, −1.269, 11.791, −0.866, −1.080, 11.730, −0.653,
−1.086, 11.731, −0.658, −1.269, 11.791

Cov(1,66) =

1.391, −1.679, −2.765, 1.191, −1.685, −2.897, 1.472, −1.671, −2.666, 1.191,
−1.685, −2.897, 1.191, −1.685, −2.897, 1.191, −1.685, −2.897, 1.191, −1.685,
−2.897, 1.191, −1.685, −2.897, 1.191, −1.685, −2.897, 1.191, −1.685, −2.897,
1.191, −1.685, −2.897, 1.191, −1.685, −2.897, −1.921, −0.892, −6.582, −1.921,
−0.892, −6.582, −2.298, −0.933, −6.326, −2.290, −0.930, −6.331, −1.921, −0.892,
−6.582, −1.921, −0.892, −6.582, −3.571, −0.864, 9.626, −3.946, −0.754, 9.214,
−3.942, −0.756, 9.219, −3.571, −0.864, 9.626

Cov(1,67) =

−2.170, 1.515, 2.277, −2.341, 1.524, 2.184, −2.131, 1.538, 2.363, −2.341,
1.524, 2.184, −2.341, 1.524, 2.184, −2.341, 1.524, 2.184, −2.341, 1.524,
2.184, −2.341, 1.524, 2.184, −2.341, 1.524, 2.184, −2.341, 1.524, 2.184,
−2.341, 1.524, 2.184, −2.341, 1.524, 2.184, 4.736, 2.189, 3.840, 4.736,
2.189, 3.840, 4.474, 2.156, 4.016, 4.481, 2.159, 4.012, 4.736, 2.189,
3.840, 4.736, 2.189, 3.840, 7.222, −1.265, −3.571, 5.923, −1.184, −3.893,
5.923, −1.186, −3.891, 6.222, −1.265, −3.571, 68.954

Cov(1,68) =

−3.220, 2.398, 4.478, −3.112, 2.395, 4.537, −3.273, 2.388, 4.408, −3.112,
2.394, 4.537, −3.112, 2.394, 4.537, −3.112, 2.394, 4.537, −3.112, 2.394,
4.537, −3.112, 2.394, 4.537, −3.112, 2.394, 4.537, −3.112, 2.394, 4.537,
−3.112, 2.394, 4.537, −3.112, 2.394, 4.537, −2.601, 7.610, −1.699, −2.601,
7.610, −1.699, −2.389, 7.632, −1.844, −2.394, 7.630, −1.841, −2.601, 7.610,
−1.699, −2.601, 7.610, −1.699, −1.269, 12.788, −0.866, −1.080, 11.730, −0.653,
−1.086, 11.731, −0.658, −1.269, 11.791, −0.866, −1.269, 21.764

Table B-2 (cont'd).

Cov(1,69) =									
1.391,	−1.679,	−2.765,	1.191,	−1.685,	−2.897,	1.472,	−1.671,	−2.666,	1.191,
−1.685,	−2.897,	1.191,	−1.685,	−2.897,	1.191,	−1.685,	−2.897,	1.191,	−1.685,
−2.897,	1.191,	−1.685,	−2.897,	1.191,	−1.685,	−2.897,	1.191,	−1.685,	−2.897,
1.191,	−1.685,	−2.897,	1.191,	−1.685,	−2.897,	−1.921,	−0.892,	−6.582,	−1.921,
−0.892,	−6.582,	−2.298,	−0.933,	−6.326,	−2.290,	−0.930,	−6.331,	−1.921,	−0.892,
−6.582,	−1.921,	−0.892,	−6.582,	−3.571,	−0.864,	10.626,	−3.946,	−0.754,	9.214,
−3.942,	−0.756,	9.219,	−3.571,	−0.864,	9.626,	41.350,	−0.864,	57.894	